

Biomimetic technique for adhesion-based collection and separation of cells in a microfluidic channel

Wesley C. Chang,* Luke P. Lee and Dorian Liepmann

Received 12th January 2004, Accepted 7th April 2004

First published as an Advance Article on the web 26th May 2004

DOI: 10.1039/b400455h

A basic step in many biological assays is separating and isolating different types of cells from raw samples. To better meet these requirements in microfluidic devices for miniature biomedical analytical systems, an alternative method for separating cells has been devised by mimicking the physiological process of leukocyte recruitment to blood vessel walls: adhesive cell rolling and transient tethering. Reproducing these interactions for cells on surfaces of microstructured fluidic channels can serve to capture and concentrate cells and even to fractionate different cell types from a continuously flowing sample. To demonstrate this principle, two designs for microstructured fluidic channels were fabricated: an array of Square pillars and another with slender, Offset pillars. These structures were coated with E-selectin IgG chimera and the interactions of HL-60 and U-937 cells with these structures were characterized. With inflow of fluidic cell suspensions, the structures were able to efficiently capture and arrest cells directly from the rapid free stream flow. After capture, cells transit through the channel in three phases: cell rolling, cell tethering, and transient re-suspension in free stream flow before re-capture. Under these interactions, captured cells were enriched several hundred-fold from the original concentration. Additionally, among collected cells, the difference in flow-driven, adhesion-mediated cell transit in the Square design suggested that the two cell types could at least be partially fractionated.

1 Introduction

One of the fundamental steps in many biological analyses is the separation of different cell types from a raw, heterogeneous sample such as blood. Often, the desired cell population must not only be separated but also enriched, or concentrated, well beyond original volumetric number densities in the raw sample. Conventional methods for cell separation take advantage of differences in various physicochemical cell properties.¹ Separations by physical properties are usually based on differences in cell size and density^{1,2} and have even included differences in cell stiffness.^{3,4} However, these differences are often slight and difficult to discern among different cell types. Immunological techniques, such as fluorescence-based flow cytometry (FACS), magnetic cell labeling (MACS), and affinity chromatography, have therefore become mainstays in clinical laboratory due to their high specificity and their broad applicability.¹ Such techniques have also been implemented successfully in microfluidic devices.^{5–7} The use of antibody-mediated immobilization or labeling, however, generally requires some preparatory and incubation time periods. Additionally, ancillary systems for actuation and detection, which are often large and elaborate, must accompany the central sample handling device. Then, following the separation step, cells must be post-processed, sometimes requiring the removal of labeling. These steps add additional processing time and reagents and may hurt process yield and can sometimes be harmful to the cells themselves. For

microfluidic devices, one alternative separation technique is dielectrophoresis, used either alone or in conjunction with another method.^{8–11} This technique, while effective in many cases, does adversely affect cell viability. The development of miniature bio-analytical systems will therefore continue to benefit from the exploration of new, elegant cell separation techniques that can serve to augment or even supplant cumbersome traditional techniques.

This work introduces an alternative method for collecting and separating cells by harnessing the natural, physiological mechanism by which blood vessels recruit leukocytes and other cell types to particular sites in the body, such as sites of injury or inflammation. At such sites, during an inflammatory response, blood vessels present a special class of adhesion proteins on their luminal surfaces to the passing blood.^{12–15} These specialized proteins, which include the selectin family, exhibit unusual biophysical properties that enable them to abruptly and selectively capture and arrest fast-moving white cells that bear complementary ligands, but because the adhesion bonds dissociate readily under mechanical loading, these adhesions do not firmly immobilize the cells.^{16–19} These adhesions have therefore been designated as “transient” adhesions. Such properties enable the adhesion proteins to substantially, selectively enrich targeted white cell types. But under fluid shear from passing blood flow, cells roll slowly along the luminal surfaces. Transient adhesions can now be exploited *in vitro* for high-throughput separation of white blood cells in a microfluidic device. Targeted cells can be captured and enriched in such a device, and among adherent cells, different cell types generally have different adhesiveness

*wchang@silicon.eecs.berkeley.edu

for the various adhesion proteins, usually resulting in different transit speeds under a given fluid shear.²⁰ This difference in affinity among different cells can provide a mechanism for chromatographically separating different adherent cells based on the differences in adhesion-mediated cell transit. Subsequently, because of high bond association rates and since many blood-borne cells constitutively express ligands for one or several of the rolling adhesion proteins, no preparatory or incubation steps are required to label or immobilize the cell; adhesion forms quickly, and cells can be readily plucked from flowing suspension under mechanical loading. Following the cell separation, minimal “destaining” or cell removal processing would be required, since the adhesions are “transient” and are thus easily reversible under mechanical loading and disruption of the Ca²⁺-mediated adhesion.

The implementation of this proposed biomimetic concept for cell separation has been envisioned as a microfluidic channel containing arrays of micropillars with characteristic spacings that are somewhat larger than the size of cells. Such spacing is intended to avoid non-adhesive, mechanical restraining or disruption of cell motion but not so large as to allow many cells to pass freely without coming into contact with a surface. Adhesion proteins, such as a selectin, are immobilized on the surfaces of the microchannel and micropillars, with raw fluid samples containing suspended cells rapidly flowed through the channel. Cells constitutively bearing ligands for the immobilized proteins would be captured and arrested from the passing sample by the protein-laden surfaces of the flow channel and restricted to slowly transit down the length of the channel, maintaining adhesive interactions with the surfaces. This scheme is intended to perform three basic functions: (1) selective capture of targeted cells suspended in continuous, rapid flow; (2) enrichment, or volumetric concentration, of these cells within the microchannel; and (3) among adherent cells that are captured and enriched, chromatographic fractionation of different cells types based on differential speeds of flow-driven transit through the channel. In this study, the proposed technique was demonstrated with two prototype designs for micropillar arrays using E-selectin-based adhesion and by characterizing the flow-driven, adhesion-mediated dynamics of HL-60 cells. The adhesion-mediated transit of a second cell line, U-937, was also measured as a comparison to the HL-60 cells.

2 Methods and materials

Test structures

The “separation columns” consisted of microfluidic flow channels containing micropillars to maximize surface area for capture of passing cells (Fig. 1). The provision for micropillar arrays maximizes the surface area presented to the passing cells. Two different microstructures were studied: a “Square array” of 25 × 25 μm square posts, spaced 25 μm apart; and an alternating array, called the “Offset array”, of thinner pillars (35 × 10 μm), spaced 30 μm but with successive downstream rows offset 15 μm in the cross-stream direction (Fig. 1). Test structures were fabricated in silicon using deep reactive ion etching (DRIE). Each array was housed in a

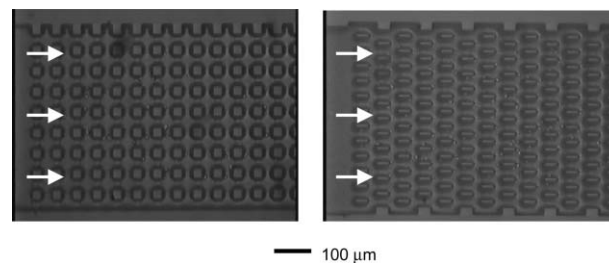


Fig. 1 Microstructured flow channels (top views). Square (left) and Offset (right). The structures were fabricated with deep reactive ion etching (DRIE). These views of the microchannels are seen through the top coverglass. Downstream flow is in the left-to-right direction, and “height” is along the axis into the image. The depth of the channels was 40 μm.

10 mm long by 500 μm wide by 40 μm deep trench bounded at either end by reservoirs with through-substrate access holes. Surfaces were immersed in piranha (mixture of H₂SO₄ and H₂O₂) to clean and to promote the growth of native silicon dioxide. Flow structures were then sealed with anodic bonding of thin pyrex glass. Characterization of cell-free fluid flow through these structures was performed experimentally with digital particle image velocimetry (DPIV) and computational fluid dynamics (CFD) using the CFDRC-ACE+ package (CFD Research Corporation, Huntsville, AL), which provides capabilities for generating grids for model geometries and performs numerical computation of fluid mechanical phenomena using the finite volume method.²¹

Protein immobilization

A water-soluble human E-selectin IgG chimera (Glycotect, Inc., Rockville, MD) was used as the adhesion protein in this demonstration. The procedure for physisorbing selectin IgG proteins on the microfabricated surfaces was based on established protocols for glass substrates:^{22–24} a 1.0 μg mL⁻¹ solution of E-selectin IgG in phosphate buffered saline (PBS) was perfused into the microfabricated channels and incubated in the channels at room temperature for 2 h. The test structure was then washed with a 3% solution of fetal bovine serum in PBS and then “blocked” for 1 h with this solution. Cell interaction with the Fc segment of the chimera was blocked by the incubation of 2 μg mL⁻¹ of anti-Fc F(ab')₂ antibody (Biosdesign, Inc., Saco, ME) for 30 min prior to flow testing. This same concentration of the anti-Fc antibody was also added directly to the cell suspensions used during flow experiments.

Prior to performing the actual adhesion experiments, some preparatory flow experiments were performed both to observe the behavior of non-adherent cells and to verify that any adhesion observed with HL-60 and U-937 cells were due to the selectins. With non-adherent cells (suspended fibroblasts), no adhesive interactions were observed with the pillar array, and the cells were carried away rapidly by the flow. Conversely, using HL-60 and U-937 cells in the absence of the adsorption of E-selectin-IgG (but including all other sample preparation steps) also resulted in no adhesive interactions, confirming that there were no non-specific adhesive interactions between these cells and the microchannel.

Cell lines

The cells used in this study were the HL-60 and the U-937 myeloid cell lines (ATCC), both bearing ligands for E-selectin. These cells were chosen because they are widely available, hardy and easy to maintain. Both cell types were maintained at 37 °C with 5% CO₂/95% air and in RPMI-1640 media supplemented with 10% fetal bovine serum (FBS) and 1% sodium pyruvate. Flow testing used cells suspensions of 100,000 per mL in the RPMI-1640 media with the anti-Fc antibody added.

Flow experiments

A syringe pump (Cole Parmer) with gas-tight glass syringe delivered the 100,000 cells mL⁻¹ suspension to the device at a flow rate of 1.0 μL min⁻¹. The flow of cell suspension through the microchannels was viewed through the pyrex coverslide with a microscope, and motion video of these flows were recorded.

Cell capture and enrichment

To determine the effectiveness of the micropillar arrays in capturing and enriching cells from free stream flow, high-speed, laser induced fluorescent images of the flow structures were captured in rapid succession as suspensions of labeled HL-60 cells (stained with SYTO 82, Molecular Probes, Eugene, OR) were introduced into the device and pumped through the flow channels at the explicit flow rate of 1.0 μL min⁻¹. This procedure allowed the collection of discrete, streak-free images of cells at short time intervals as they transited the flow channel and adhered to the surfaces or travelled in the free stream, allowing individual cells to be counted and adherent cells to be distinguished from cells carried with the free stream.

Effectiveness of cell capture was determined by counting the proportion of free stream cells that were captured by surfaces in the flow structure during the first 700 μm of channel length *versus* cells that transit through this length without adhesive interactions. The proportion of incoming cells captured was compiled for the first minute (60 s) of operation following initial introduction of sample and again for the third minute of operation to assess whether the presence of increasing density of adherent cells on the pillar arrays affected the subsequent capture of new incoming cells.

Cell enrichment was calculated based on the concentration of cells in the flow channel, which was determined by counting the cells in the device from the captured images. The number of cells was counted in the images marking 30 s intervals from 0 to 4 min following the initial introduction of sample.

Cell transit

Average transit speeds of the cells were determined by dividing the transit distance through the video frame (700 μm) by the total transit time. Cells that adhered and rolled for some distance and then detached from the channel surfaces before completion of transit through the frame were also counted and tallied as “detached” cells.

The distribution of cell transit speeds can in some cases be fitted to an Exponentially Modified Gaussian (EMG), a

mathematical template commonly used to characterize asymmetric statistical distributions.²⁵ It has the form:

$$f(x) = \frac{1}{2\tau} \exp \left[0.5 \left(\frac{\sigma}{\tau} \right)^2 - \left(\frac{v - v_0}{\tau} \right) \right] \left[\operatorname{erf} \left(\frac{1}{\sqrt{2}} \left(\frac{v_0}{\sigma} + \frac{\sigma}{\tau} \right) \right) + \operatorname{erf} \left(\frac{1}{\sqrt{2}} \left(\frac{v - v_0}{\sigma} - \frac{\sigma}{\tau} \right) \right) \right] \quad (1)$$

where v represents the transit speed of the cell, σ is a constant representing the broadness of the distribution, and τ is a characteristic constant of the exponential decay function. The resolution R_s between two distributions, which is a measure of how distinguishable the distributions are, can be defined as:

$$R_s = \frac{v_{02} - v_{01}}{\frac{1}{2}(pw_1 + pw_2)} \quad (2)$$

where v_0 is the speed at the peak of the distribution of transit speeds and pw is the width of the peak, which in this study was defined as the width of the distribution standing more than 10% of the peak height.

3 Results and discussion

3.1 Characterization of flow in micropillar arrays

The characterizations of the micropillar (Fig. 2) arrays showed that with the Square pillars, the larger cross sections and linear arrangement of pillars resulted in straight streamlines and a large region of sluggish flow behind each pillar: the maximum flow speed directly behind each pillar was severely diminished from the average speeds in the passage between the lateral surfaces of the pillars. By contrast, the arrangement of pillars in the Offset geometry generated curved, non-linear streamlines, which weaved back and forth between the offset pillars, and the slender cross-sections of the pillars did not promote the formation of sluggish flow regions behind the trailing (downstream-facing) surfaces. Under a flow rate of 1.0 μL min⁻¹, shear stresses of 5.9 dynes cm⁻² was generated on the bare lateral surface of the Square pillars and 3.1 dynes cm⁻² was generated on the bare Offset pillars. However, hydrodynamic resistance, as determined by CFD simulation, of the two flow structures were similar, meaning that similar driving pressures would produce the same volumetric flow rates through both of the flow structures.

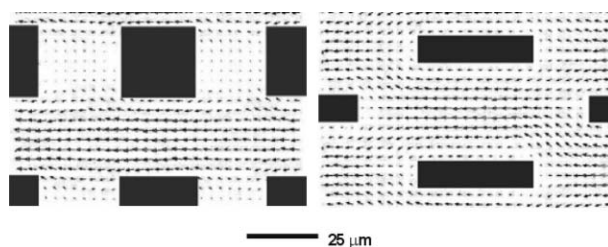


Fig. 2 Vector plot of measured velocity field in the microstructures using DPIV. (right to left). In the Square geometry, the streamlines are straight, while in the Offset geometry, the streamlines are curved and weave around the pillars. Additionally, the sluggish flow region is evident behind the Square pillars can be clearly recognizable, whereas the slim Offset pillars do not exhibit this sluggish region.

3.2 Initial cell capture from free stream

An unusual property of selectin-mediated adhesion is the possibility of sudden cell arrest from rapid transit in the fluid suspension due to high bond association rates, which allow selectin and ligand to bond after very brief though close apposition. In this study, capture and arrest of HL-60 cells occurred along surfaces in both of the microchannel designs (Fig. 3 and 4), although the flow geometry did profoundly affect the efficiency of capture (proportion of cells captured *vs.* cells eluting through a particular segment of channel). Under dilute cell concentrations (the first minute of sample capture), when cell density in the structures was low, the pillars of the Offset array more effectively captured cells flowing into the array. At $1.0 \mu\text{L min}^{-1}$, about 95% ($n = 4$) of cells were captured over the first $700 \mu\text{m}$ length of the channel with Offset pillars, while 72% ($n = 4$) were captured in the Square channels. When the devices became filled with adherent cells, however, the capture rate for the Square array improved markedly, achieving efficiencies comparable to the Offset geometry. Capture rates in the Squares geometry measured during the third minute of operation—when the average cell enrichment was around $150\times$ and cell concentration was about $15 \text{ million cells mL}^{-1}$ —reached between 85 and 94% ($n = 4$) for the flow rate of $1.0 \mu\text{L min}^{-1}$. (Fig. 4)

A noteworthy attribute of these results is the correlation of the higher capture rate with fluid flow characteristics consisting of curved and weaving streamlines. This flow field, seen in the Offset structure, would most likely carry suspended cells on curved and weaving trajectories. By contrast, flow through a bare Square array, with its straight geometry, would carry the cells linearly through the channels between rows of pillars. With increasing cell densities in the Square array, however, the straight streamlines of the flow would invariably be disturbed, creating irregular flow fields, with more curved streamlines, to negotiate around adherent cells. This presumed transition in the flow field was also associated with higher cell capture rates. Since cell capture is promoted by close apposition of cells to micropillar surfaces (protein and ligand must approach each other within a distance on the order of the size of the adhesion molecules), it would seem that curved trajectories created opportunities for cells to contact the surfaces of the micropillar arrays. This may be due in part to the slight difference in density between cell and suspending media, resulting in the slight deviations of cells from following streamlines that are curved, allowing them to more easily encounter surfaces. However, this hypothesis regarding the effect of the shapes of

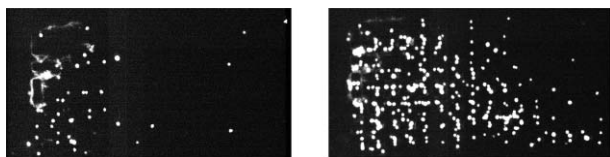


Fig. 3 HL-60 cells captured on the Square lattice. Two views taken 2 min apart show cells (white) accumulating on the surfaces of the microchannel. Cells were captured from a flowing suspension and transited slowly down the length of the channel (flow from left to right).

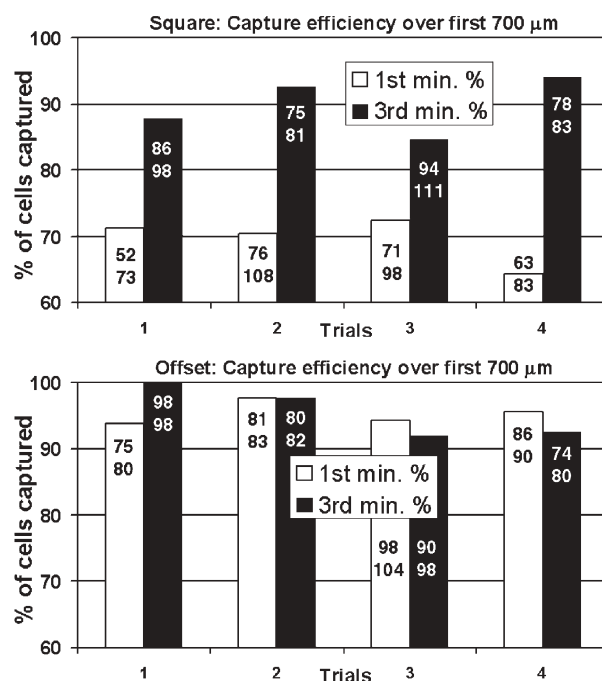


Fig. 4 Capture efficiency for Square and Offset geometries. Percentage of cell captured along the first $700 \mu\text{m}$ length of the fluidic channel. Numbers in each bar indicate the actual number of cells captured (top number) and the total number of cells entering the flow chamber (bottom number). In the Square geometry, the initially straight streamlines do not favor cell capture compared with the curved streamlines of both the Offset geometry and the Square geometry after being populated with cells.

streamlines in promoting cell-to-surface apposition remains to be demonstrated and characterized explicitly.

3.3 Adhesion-mediated motion through microchannels

As fluid flowed continuously through the microchannels, adherent cells were driven by the fluid shear and consequently transited slowly down the length of the microstructured channels. Based on experimental observations and measurements, it was determined that the adhesion-mediated dynamics of the cells transiting among the micropillar lattices involved three distinct phases (Fig. 5): (1) fluid shear-driven rolling along the surfaces of the micropillar or the microfluidic channel; (2) transient immobilization of the cell on the trailing (rear-facing) surface of the pillars, the duration of which is governed by the tension-dependent dissociation kinetics of selectin-ligand bonds; and (3) free, suspended transport following dissociation of the cell from the trailing surface and before recapture on a surface downstream and recycling through the three phases. Overall flow-driven, adhesion-mediated dynamics of cells through the channel was determined by the behavior of cells in each of these three regimes, which was governed by the fluid mechanics and channel geometry. The cell transit speeds determine how effectively the microstructures enrich (concentrate) local number densities of cells. In the meantime, the widths of the statistical distributions of cell transit speeds, relative to the difference in means,

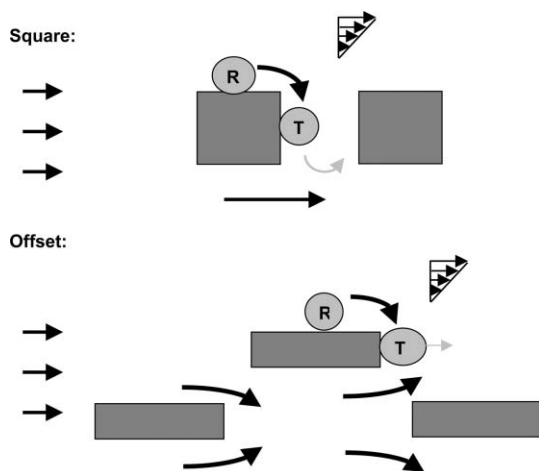


Fig. 5 Phases of cell dynamics. When adhering to the lateral surfaces of the micropillars (R), cells experience fluid shear in the tangential (relative to the surface) direction and consequently roll slowly. Once the cells reach the trailing surface of the pillars, fluid shear loading pulls the cells perpendicularly away from the pillar (T). Here, the cell tethers for a short period before detaching from the surface and re-entering the free suspension. In the Square array, due to the sluggish flows behind pillars, cells re-entering the suspension from tethering are almost always re-captured by the next pillar immediately downstream (gray).

determine whether and how effectively different adherent cell types can be chromatographically distinguished.

Cell rolling. When subjected to tangential fluid shearing, an adherent cell rolls along the surface because the fluid shear induces a torque and force on the adherent cell, bringing forward parts of the cell membrane in contact with the surface, where new selectin-ligand bonds to form, but inducing old bonds to dissociate along the trailing edge due to mechanical tension. During this entire process of “dynamic adhesion”, the cell remains associated with the underlying substrates *via* selectin-ligand bonds, but the bonds are continually turned over to accommodate the rolling motion.^{17,26}

Under continuous fluid flow through the microchannels, cells adhering on the lateral micropillar surfaces exhibited this rolling motion, driven by fluid shear. Quantifying the rolling speeds among the micropillars was somewhat complicated since the forces incident on a cell depended on its position along both the vertical and downstream axes. Therefore, a baseline relationship between rolling speed and fluid mechanical loading was established by comparing shear loading experienced by cells adherent to a flat surface of same composition as the fabricated channels and under quasi-Couette flow. Loading of cells rolling on flat surfaces was calculated using the analytical derivations of Goldman *et al.*,^{27,28} while the resulting rolling speed was measured experimentally. With this baseline relationship, it would be possible to estimate average rolling speeds and variations in rolling speeds by knowing just the fluid mechanical loading experienced at various locations in the micropillar lattice.

Cell tethering. During transit through the microstructure, adherent cells are invariably swept behind the pillar and spent

short periods of time tethering to the trailing (relative to the flow direction) surfaces of the pillars. Once situated behind these pillars, the cells were subject to a different type of mechanical loading: instead of the tangential fluid shearing, as was experienced on most other surfaces of the microchannel, the net shear from the flow field actually pulled the cell away from the surface, subjecting all of the adhesive bonds to mechanical tension. Tethering with the bonds under tension was therefore always temporary, and the cells always dissociated eventually from the pillar surface. Experimental measurements of the cell tethering durations showed that tethering lasted about twice as long on the Square pillar than on the Offset pillar. In the Square geometry, the median duration was 12.5 s; in the Offset geometry, median duration was 5.5 s (Fig. 6).

The duration of tethering of cells on the trailing surfaces of the pillars depended on the magnitude of tension force exerted by the fluid shear on the cell. This force influences the dissociation kinetics of the adhesion bonds mediating the tethering. CFD modeling determined that higher tension forces were incident on the cells tethering on the trailing face of the slender pillar of the Offset geometry. At the center, under operating flow rate of $1.0 \mu\text{L min}^{-1}$, a cell experienced

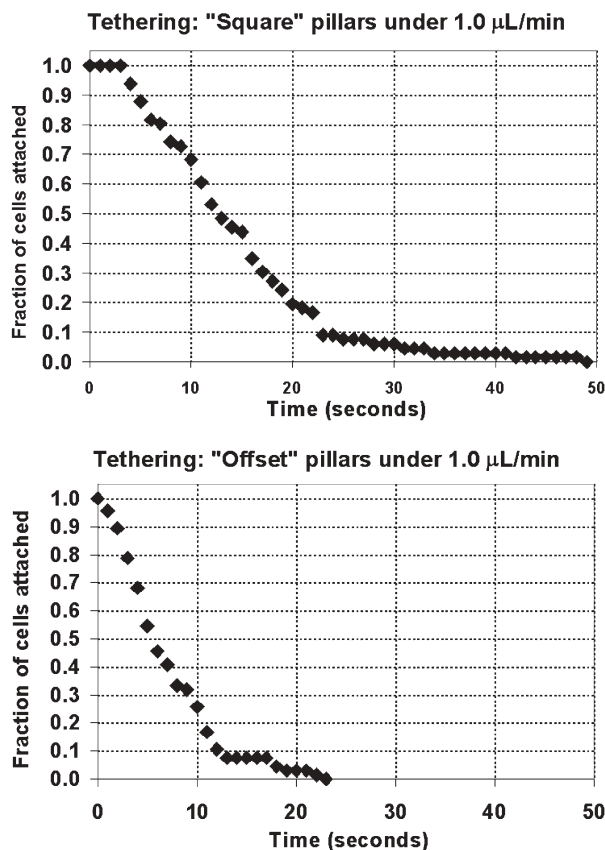


Fig. 6 Fraction of cells remaining adherent vs. duration of cell tethering. In both types of pillars, the duration of cell tethering is distributed over tens of seconds. The durations are notably longer in the Square array, owing to the smaller tension force experienced by the tethering cells there. In the Square array, the tethering cell experienced only 5.8 to 11 pN of force; in the Offset array, the cell was exposed to 58 to 117 pN.

117 pN of tension, while along the channel floor or top, the tension force was still 68 pN. Meanwhile, on the trailing surface of the Square pillar, under the same flow rate, a cell experienced only 11 pN at the centered position on the pillar, and a mere 5.8 pN at the centered floor or top position. The roughly factor of 10 difference between the tethering forces present in the Square vs. Offset geometries was responsible for the factor of 2 difference in the tethering durations, a result supported by theoretical analysis of the bond kinetics using a probabilistic model of dissociation kinetics.²⁹ It should be noted that the factor of two uncertainty in tension force for each geometry translates into a relatively smaller difference in tether duration in each case.

Suspended transport. Following tethering, the cell adhesion breaks, as all the bonds have by then dissociated, and the cell briefly enters the suspension to be carried away by the fluid flow. However, there was an important difference observed between the suspended transport of cells in the two array designs. In the Square array, the cells, following tethering and detachment, simply jumped to the immediate pillar downstream to begin the rolling process anew. In the Offset array, however, cells entered the free stream between pillars and were carried arbitrary distances downstream before recapture by the micropillar array. This extended residence time in the free stream for the Offset array increased the average cell transit speed and widened the statistical distribution of transit speeds relative to the cell transit speeds in the Square array (Fig. 7). Transit for most cells in the Square array was dominated by the rolling and tethering phases, with the suspended phases lasting only the brief transfer from one pillar to the next,

though a notable fraction (10%) of the cells did enter the free stream and were carried away beyond the 700 μm viewing window. It should be noted that since tethering cells re-entered the free stream from the trailing surface of the pillar, they remain in the sluggish flow region and thus are mostly recaptured on the next pillar; this contrasts with the initial capture of entering cells, which mostly travel in the space between the lateral surface of the pillars, making them much more difficult to capture.

Composite transit. Since the overall transit of cells through the micropillar arrays consisted of the three mechanisms of rolling, tethering, and suspended transport, a numerically derived prediction of the overall statistical distribution of transit speeds was constituted from: (1) statistical distribution of cell rolling speeds determined by correlating CFD calculated fluid mechanical loading of cells in the lattices and empirically established relationship between shear loading and rolling speed of cells on flat substrates; (2) experimentally determined distribution of cell tethering durations; and (3) statistical distribution of distances cell travelled in suspended phase. First, the number density function for cell rolling speed was transformed to a density function with respect to the duration time of cell rolling on a single pillar. For both the Square and Offset flow geometries, this density function was then convoluted with the number density function of cell tethering duration to yield a composite density function for the total duration of the rolling and tethering phases. For the Square geometry, this function corresponded to the statistical distribution of total time needed to transit the 25 micron pillar—rolling for this distance followed by stationary tethering; for the Offset geometry, the analogous distance was 35 microns. Incorporating the third phase of cell transit, the free suspension transit, required different approaches for the two geometries owing to the difference in behavior of the free stream phase. In the Square array, all cells were prescribed to travel the exact distance between pillars, while for the Offset array, the recapture distribution was prescribed to be an exponential decay function corresponding to 95% capture over 700 μm , based on experimental measurements. For this analysis, the suspended phase for both geometries was deemed to take zero time, since the duration from cell detachment (after tethering) to recapture in both geometries, regardless of distance travelled, occurred very rapidly and took only a small fraction of a second. Thus, for the Square array, where the suspended transport almost always took the cells to the next pillar downstream, the additional distance of exactly 25 microns was added to represent the distance travelled in suspension, and no additional time was needed. The density function for the overall cell transit speed was therefore produced by transforming the density function of the rolling-plus-tethering duration with the understanding that a total of 50 microns was traversed during this duration. For the Offset geometry, however, the rolling-plus-tethering density function had to be considered in conjunction with the statistical distribution of suspended transit distances. An additional transformation was performed to combine the two statistical distribution functions to generate the composite distribution function of overall cell transit speeds. The numerically derived

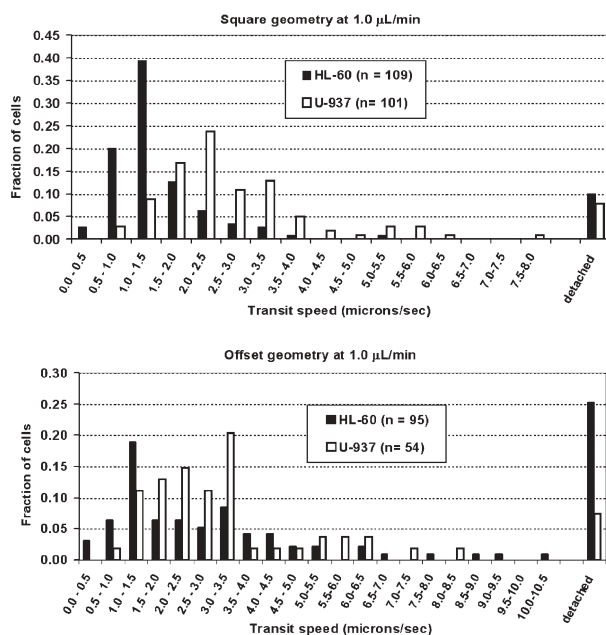


Fig. 7 Overall transit speeds of cells through the Square and Offset flow geometries at $1.0 \mu\text{L min}^{-1}$. Differences in transit speed between the HL-60 and U-937 cells can be easily discerned in the former design, though there is some overlap in the statistical distribution of transit speeds. In the latter design, however, the transit speeds could not be meaningfully distinguished between the two cells.

HL-60 transit speed distributions (Fig. 8) for suspension flow rate of $1.0 \mu\text{L min}^{-1}$ corresponded to the distributions measured experimentally in both geometries. However, for both arrays, the predicted distribution slightly overestimated the actual distribution of transit speeds. Actual transit speeds were dependent on the positioning of cells along the depth of the channels, with cells near the top or bottom travelling somewhat slower due to the slower local flow fields. A more complete theoretical reconstruction would account for the statistical variation in vertical cell position. While this methodology for calculating the statistical distribution of cell transit through an array of micropillars is not entirely theoretically based, it offers a systematic way to mathematically predict or at least estimate cell behavior when contemplating different designs and known flow conditions.

3.4 Cell enrichment

HL-60 cell concentrations were greatly enriched (Fig. 9) from the original concentration in both devices as cells entering the channel accumulated on the lattice surfaces, but the Square geometry was able to collect and maintain a higher concentration of cells. In the Square geometry, cell concentrations in the

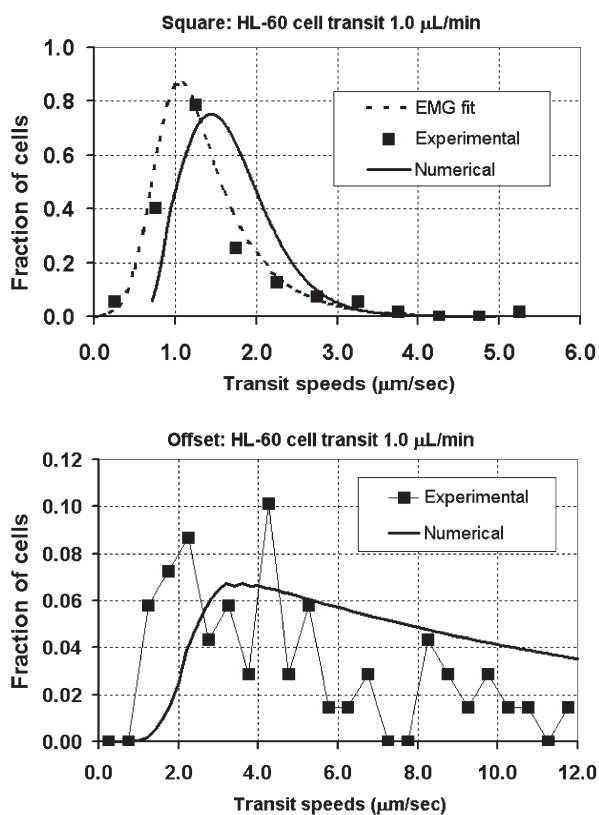


Fig. 8 Based on knowledge of the statistical distributions of the individual phases of rolling, tethering, and suspended transport, a composite distribution for overall HL-60 cell transit speed through the pillar arrays can be constructed numerically based on the knowledge of the statistical distributions of the three individual phases of cell rolling, tethering, and free suspension. The biggest difference between the cell transit distributions for the two structures can be attributed to the time spent in the suspended phase of cell transit.

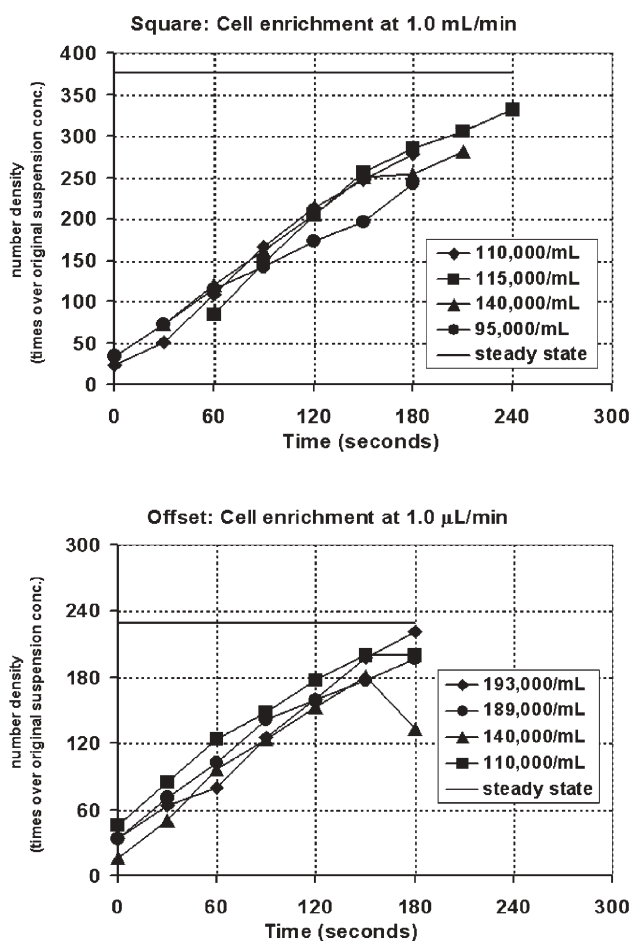


Fig. 9 HL-60 cell enrichment vs. time for both micropillar arrays. In the Square array, the enrichment of cells reached almost 400 times (steady state), while for the Offset array, cells were concentrated to less than 240 times the original concentration. These measurements were performed for initial cell concentrations of about $100,000 \text{ cells mL}^{-1}$. (Legend indicates initial cell concentration.)

first $700 \mu\text{m}$ of channel rose to a steady state of 377 ± 91 ($n = 4$) times during operation at $1.0 \mu\text{L min}^{-1}$. The Offset geometry produced somewhat less enrichments at the high flow rate, with cells concentrations reaching 229 ± 42 ($n = 4$) fold steady state at $1.0 \mu\text{L min}^{-1}$ flow. In both structures, overall cell concentration in the channel increased roughly linearly with time over the first $3\frac{1}{2}$ min and until steady state was attained. Naturally, initial capture of cells was concentrated towards the entrance of the channel, so that the upstream accumulation of cells occurred faster, and cell concentrations reached steady state sooner than in downstream regions of the channel. As time progressed, steady state cell concentrations were attained by the structures progressively downstream. This pattern of cell accumulation and enrichment was seen in high speed images of fluorescence-labeled cells transiting the flow channel (Fig. 3).

Cell enrichment was greater with the Square structure, since this flow geometry more effectively slowed cells under continuous flow, with fewer cells detaching. This flow geometry more effectively slowed the cells due to the presence of large regions in which fluid flow is substantially slowed.

With the Offset pillars, however, the absence of sluggish flow regions behind pillars shortened tethering and limited their accumulation. Additionally, cells in the Offset geometry generally travelled further in the free stream phase between the tethering and recapture events. Cells therefore transited faster through the flow channel and could not be enriched to the concentration achieved with the Square geometry.

3.5 Differential cell transit speeds: possibility for chromatographic fractionation

To demonstrate the possibility for chromatographic fractionation of cells, HL-60 and U-937 cells travelled at measurably and significantly different speeds in the Square geometry (HL-60 vs. U-937, 1.4 ± 0.8 vs. $2.7 \pm 1.4 \mu\text{m s}^{-1}$, $p \ll 0.001$, unpaired t -test), though there was some overlap between the statistical distributions of transit speeds (Figs. 7 and 10). This difference has a chromatographic resolution of $R_s = 0.31$ and may provide the basis for partially fractionating these two cell populations using this particular microstructure with E-selectin. In the Offset geometry, however, the distribution of transit speeds for both cell types was much wider than in the Square geometry, owing largely to the dominant nature of the suspended phase of cell transit. Thus, no significant difference in transit could be discerned between the two cell types (HL-60 vs. U-937, 3.7 ± 4.0 vs. $3.3 \pm 2.1 \mu\text{m s}^{-1}$, $p = 0.088$, unpaired t -test), as the wideness of transit distributions obscured the intrinsic difference in the adhesion-mediated transit dynamics between the two cell types.

As a comparison, under adhesive cell rolling on flat substrates and under quasi-Couette flow field, HL-60 cells was found on average to roll at a consistently slower speed than the U-937 cells, which usually travelled at roughly 1.5 times the speed of HL-60 at any given shear stress over the range of shear stresses studied. However, despite the differences in average rolling speeds, the distributions of speeds of these cells did also overlap to some extent. This difference in transit speeds was similar to the difference in cell transit with the Square pillar array.

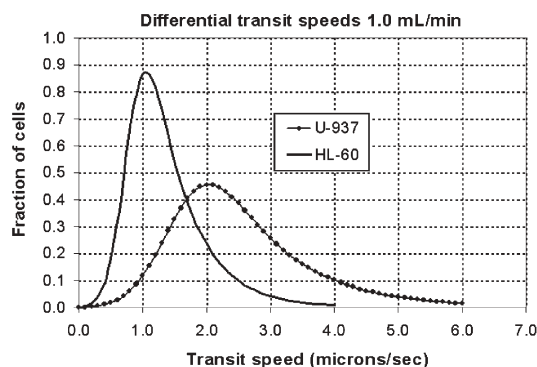


Fig. 10 EMG-fitted distribution curves for the HL-60 and U-937 cell transit speeds in the Square Array. The distributions are discernable and partial separation of the cells is possible. The chromatographic resolution was $R_s = 0.31$. This is adequate only for partial fractionation of the HL-60 and U-937 cells.

3.6 Limitations of the current demonstration

Although this study provided a clear demonstration of the feasibility of adhesion-based cell sorting, there were several limitations. This selection of one adhesion molecule, E-selectin, did not specifically cater to the separation of HL-60 and U-937 cells, nor were the designs of flow structures. While this work provided a rudimentary demonstration of the proposed cell collection and separation functions, it was inadequate to give a sense of the ultimate capabilities and limits of this technique, given the availability of similar adhesion proteins and wide variety of possible target cells. Also, the present method of characterization observes cell transit through only $700 \mu\text{m}$ of channel length. With this window, it was not possible to characterize the longer range statistics of suspended cell transit and recapture downstream. Furthermore, it is not clear to what extent the distribution of transit speeds for each cell type is attributable to inherent differences among individual cells within a population or to differences in the positions on the lattice in which cells transited through or simply to the statistics of adhesion. For example, cells that adhere near a corner, making contact with two perpendicular surfaces, would transit slower than cells that are adhere on just one surface (though the majority of adhesive interactions were indeed with just one surface). However, baseline quantification of cells rolling on a simple flat surface suggests that there is a large degree of scatter in rolling speeds among different individuals of each cell type. Again, this may be due to differences in individual cell or to adhesion statistics. This remains to be studied in more detail.

4 Conclusion

This study proposed and demonstrated the use of selectin-based, transient adhesions to capture, enrich, and even fractionate different types of cells in a microstructured fluidic channel. E-selectin-based adhesion was harnessed to capture and arrest HL-60 cells suspended in rapid flow through two different microstructured fluidic channels, resulting in highly enriched populations accumulated in the structured channels. Between two different cell types (HL-60 vs. U-937), the difference in transit speeds indicated that at least partial chromatographic fractionation was possible in the Square array, where the distribution of the two cell types was clearly segregated. This difference between HL-60 and U-937 cells, however, was incomplete, and highly purified samples of each would be unlikely to be obtained with the current construction and tested cell types.

In characterizing this technique, it was observed the cells undergo three basic steps during their transit down the length of the channel: adhesive rolling, tethering, and suspended transport in the free stream flow. Establishing the quantitative relationships between fluid mechanical loading of the cell and its behavior in each of the phases provided a methodology for systematically estimating the behavior of cells in any micropillar array prior to experimental characterizations. This may be a useful way to guide the refinement of this technique, to improve microchannel designs and select appropriate adhesion protein or combination of proteins for targeted cells.

Future work undoubtedly remains to more thoroughly explore the capabilities and limitations of this cell separation technique. Upcoming efforts will refine the characterization methodology used here and address the limitations in this study. Future efforts will also include devising improved flow structures, which would be designed explicitly to best utilize the three distinct phases of the dynamics of cell transit to produce the desired transit characteristics and to accentuate differences between different cell types. It will therefore be necessary to evaluate the dynamics of diverse cell types in these structures. Concurrent with this effort, the use of other selectins and similar adhesion proteins, both individually and in various combinations will yield a broad understanding of the biophysical parameters for the interactions of various adhesion proteins and combinations of adhesion proteins with potential target cells. This will permit optimal selection of proteins and protein combinations, which when combined with optimal design of flow structures, will maximize the effectiveness of cell capture and enrichment and even accentuate the chromatographic differences among different cell types.

Also to be addressed, harvesting cells following enrichment or fractionation will require some mechanism to remove the cells from the collection pillar array. Because of the transient nature of the selectin-mediated adhesion, gentle mechanical perturbation—perhaps from fluid shear directed perpendicular to the separation channel—can be used to remove the cells and transport them to a collection area. An additional consideration is that selectin-mediated bonds are dependent on Ca^{2+} ions. Chelating the calcium ions with addition of some EDTA (a common reagent) would readily disrupt the adhesion and quickly free the cells. This fast-acting process is much gentler to cells than conventional “destaining” reactions.

While it is still unclear what the ultimate capabilities and boundaries of technique will be, this approach to cell collection and separation offers several important advantages. Cells constitutively express ligands and proteins that mediate these transient adhesions and therefore require no pretreatment steps, saving time and yield. Capture of unlabeled, free-flowing cells and enrichment of these cells many fold over their original density is feasible, as was demonstrated here. Different populations can be separated simply by using fluid shear in a microfluidic channel, which serves as a microscale, chromatographic “separation column” with explicitly defined microstructures. Thus, no special devices will be needed to apply magnetic fields, electric potentials, or special optical detection methods, as will be required by conventional cell separation techniques; in particular, no special off-chip systems are needed. Devices to pump microliters of fluid would be sufficient. This proposed approach to cell separation potentially applies to a broad variety of cells and is not restricted merely to leukocytes; transient-type adhesions have been implicated in the localization of blood progenitor cells to bone marrow¹⁴ and some blood-borne cancer cells to certain tissues.^{30,31} With these advantages, the use of transient adhesions is a tantalizing technique to be implemented in micro-assay systems. In these miniaturized biological and medical laboratories, the benefits of small sample sizes, rapid sample processing, miniaturized volumes, and automation can be better realized by using cell collection and separation

methods which are elegant and rely on minimal sample processing.

Acknowledgements

This work was supported by the Defense Advanced Research Projects Agency (DARPA) FLUMES program and the Whitaker Foundation’s Graduate Research Fellowship. All devices were fabricated in the U.C. Berkeley Microfabrication Facility.

Wesley C. Chang,* Luke P. Lee and Dorian Liepmann
Berkeley Sensor and Actuator Center, University of California, Berkeley, 94720, USA. E-mail: wchang@silicon.eecs.berkeley.edu

References

- 1 *Cell Separation Methods and Applications*, ed. D. Recktenwald and A. Radbruch, Marcel Dekker, Inc., New York, 1998.
- 2 P. E. Lindahl, On the counterstreaming centrifugation in the separation of cells and cell fragments, *Biochim. Biophys. Acta*, 1956, **211**, 411–415.
- 3 R. H. Carlson, C. V. Gabel, S. S. Chan and R. H. Austin, Self-sorting of white blood cells in a lattice, *Phys. Rev. Lett.*, 1997, **79**, 11, 2149–2152.
- 4 T. A. J. Duke and R. H. Austin, Microfabricated sieve for continuous sorting of macromolecules, *Phys. Rev. Lett.*, 1998, **80**, 7, 1552–1555.
- 5 J.-W. Choi, T. M. Liakopoulos and C. H. Ahn, An on-chip magnetic bead separator using spiral electromagnets with semi-encapsulated peralloy, *Biosens. Bioelect.*, 2001, **16**, 409–416.
- 6 N. Chronis, W. Lam and L. P. Lee, A microfabricated bio-magnetic separator based on continuous hydrodynamic parallel flow, in *Micro-TAS 2001*, Monterey, CA, USA, 2001.
- 7 A. Y. Fu, H.-P. Chou, C. Spence, F. H. Arnold and S. Quake, An integrated microfabricated cell sorter, *Anal. Chem.*, 2002, **74**, 11, 2451–2457.
- 8 G. De Gasperis, J. Yang, F. Becker, P. R. C. Gascoyne and X.-B. Wang, Microfluidic cell separation by 2-dimensional dielectrophoresis, *Biomed. Microdev.*, 1999, **2**, 1, 41–49.
- 9 Y. Huang, X.-B. Wang, F. F. Becker and P. R. C. Gascoyne, Introducing dielectrophoresis as a new force field for field-flow fractionation, *Biophys. J.*, 1997, **73**, 1118–1129.
- 10 X.-B. Wang, J. Vykoukal, F. F. Becker and P. R. C. Gascoyne, Separation of polystyrene microbeads using dielectrophoretic/gravitational field-flow-fractionation, *Biophys. J.*, 1998, **12**, 3846.
- 11 J. Yang, Y. Huang, X.-B. Wang, F. F. Becker and P. R. C. Gascoyne, Cell separation on microfabricated electrodes using dielectrophoresis/gravitational field flow fractionation, *Anal. Chem.*, 1999, **71**, 5, 911–918.
- 12 K. Ley, *Inflammation: The Leukocyte Adhesion Cascade*, Charlottesville, VA, 2000.
- 13 M. B. Lawrence and T. A. Springer, Leukocytes roll on a selectin at physiologic flow rates: distinction from and prerequisite for adhesion through integrin, *Cell*, 1991, **65**, 859–873.
- 14 M. P. Bevilacqua and R. Nelson, Selectins, *J. Clin. Invest.*, 1993, **91**, 379–387.
- 15 D. Vestweber and J. E. Blanks, Mechanisms that regulate the function of selectins and their ligands, *Physiol. Rev.*, 1999, **79**, 1, 181–213.
- 16 R. Alon, D. A. Hammer and T. A. Springer, Lifetime of the P-selectin carbohydrate bond and its response to tensile force in hydrodynamic flow, *Nature*, 1995, **374**, 539–542.
- 17 K.-C. Chang, D. F. J. Tees and D. A. Hammer, The state diagram for cell adhesion under flow: leukocyte rolling and firm adhesion, *Proc. Natl. Acad. Sci. USA*, 2000, **97**, 21, 11262–11267.
- 18 D. A. Hammer and D. A. Lauffenburger, A dynamical model for receptor-mediated cell adhesions to surfaces, *Biophys. J.*, 1987, **52**, 475–487.
- 19 C. E. Orsello, D. A. Lauffenburger and D. A. Hammer, Molecular properties in cell adhesion: a physical and engineering perspective, *Trends Biotechnol.*, 2001, **19**, 8, 310–316.

-
- 20 P. H. Reinhardt and P. Kubes, Differential leukocyte recruitment from whole blood *via* endothelial adhesion molecules under shear conditions, *Blood*, 1998, **92**, 12, 4691–4699.
 - 21 CFD Research Corporation, Huntsville, Al, <http://www.cfdrc.com>.
 - 22 D. K. Brunk and D. A. Hammer, Quantifying rolling adhesion with a cell-free assay: E-selectin and its carbohydrate ligands, *Biophys. J.*, 1997, **72**, 2820–2833.
 - 23 M. B. Lawrence and T. A. Stringer, Neutrophils roll on E-selectin, *J. Immunol.*, 1993, **151**, 11, 6338–6346.
 - 24 S. R. Watson, Y. Imai, C. Fennie, J. S. Geoffroy, S. Rosen and L. A. Lasky, A homing receptor-IgG chimera as a probe for adhesive ligands of lymph node high endothelial venules, *J. Cell Biol.*, 1990, **110**, 2221–2229.
 - 25 J. P. Foley and J. G. Dorsey, A review of the Exponentially Modified Gaussian (EMG) function: evaluation and subsequent calculation of universal data, *J. Chromatogr. Sci.*, 1984, **22**, 40–46.
 - 26 D. A. Hammer and S. Apt, Simulation of cell rolling and adhesion on surfaces in shear flow: general results and analysis of selectin-mediated neutrophil adhesion, *Biophys. J.*, 1992, **63**, 35–57.
 - 27 A. J. Goldman, R. G. Cox and H. Brenner, Slow viscous motion of a sphere parallel to a plane wall—I Motion through quiescent fluid, *Chem. Eng. Sci.*, 1967, **22**, 637–651.
 - 28 A. J. Goldman, R. G. Cox and H. Brenner, Slow viscous motion of a sphere parallel to a plane wall—II Couette flow, *Chem. Eng. Sci.*, 1967, **22**, 653–660.
 - 29 C. Cozen-Roberts, D. A. Lauffenburger and J. A. Quinn, Receptor-mediated cell attachment and detachment kinetics I. Probabilistic model and analysis, *Biophys. J.*, 1990, **58**, 841–856.
 - 30 S. Aigner, C. L. Ramos, A. Hafezi-Moghadam, M. B. Lawrence, J. Friederichs, P. Altevogt and K. Ley, CD24 mediates rolling of breast carcinoma cells on P-selectin, *FASEB J.*, 1998, **12**, 1241–1251.
 - 31 D. J. Goetz, B. K. Brandley and D. A. Hammer, An E-selectin-IgG chimera supports sialylated moiety dependent adhesion of colon carcinoma cells under fluid flow, *Ann. Biomed. Eng.*, 1996, **24**, 87–89.